Supporting Information

Sulfurized Synthesis of a New Anode Material for Li-Ion Batteries: Understanding the Role of Sulfurization in Lithium Ion Conversion Reactions and Promoting Lithium Storage Performance

Yanmin Qin,[a] Zhongqing Jiang,[b] Liping Guo,[a] Jianlin Huang,[a,c] Zhong-Jie Jiang,[a,c,*] and Meilin Liu[d]

[a] Guangzhou Key Laboratory for Surface Chemistry of Energy Materials, New Energy Research Institute, College of Environment and Energy, South China University of Technology, Guangzhou 510006, P. R. China

[b] Key Laboratory of Optical Field Manipulation of Zhejiang Province, Department of Physics, Zhejiang Sci-Tech University, Hangzhou 310018, P. R. China

[c] Guangdong Engineering and Technology Research Center for Surface Chemistry of Energy Materials, College of Environment and Energy, South China University of Technology, Guangzhou 510006, P. R. China

[d] School of Materials Science and Engineering, Georgia Institute of Technology, Atlanta, GA, 30332-0245, USA

***Corresponding authors**

E-mail: eszjiang@scut.edu.cn (Z.-J. Jiang).

Contents

1. SEM and TEM images of MnO@NC and NC 3

2. TGA curve of MnOS@NSC and XRD pattern after the TGA analysis .3

3. Raman spectra of MnOS@NSC 4

4. Rate performance comparison of the MnOS@NSC with other TMO-based anode materials 5

5. Electrochemical performance of NSC and NC......................................6

6. High resolution XPS spectra of C 1s, O 1s, N 1s, and S 2p in NSC. 7

7. Total and projected DOSs of MnO_2 8

8. Comparison of the charge transfer resistance of MnOS@NSC with other MnO_2-based electrodes 8

References..9

1. SEM and TEM images of MnO@NC and NC

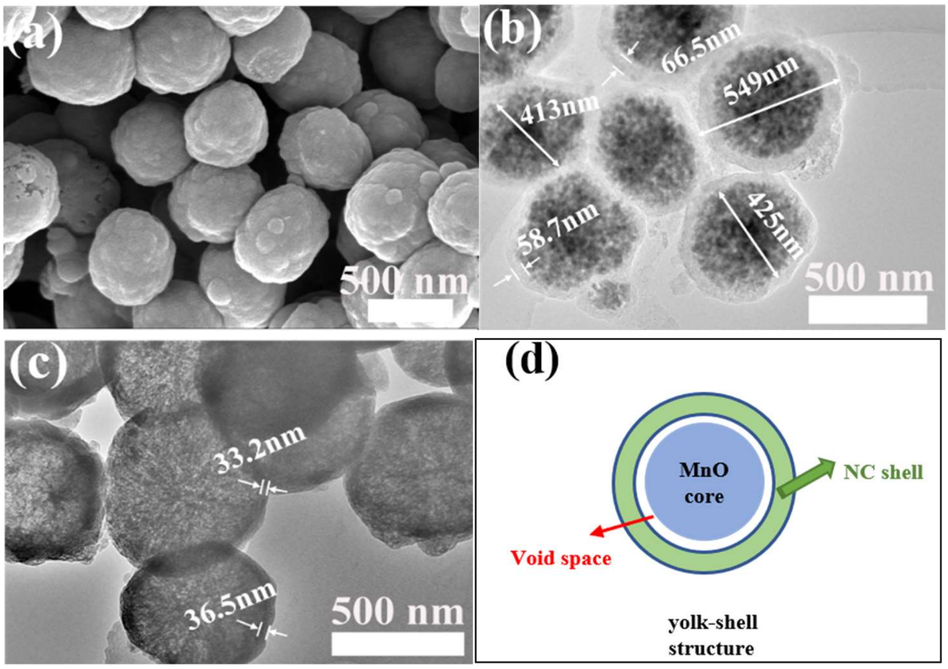

Figure S1. (a) SEM and (b) TEM images of MnO@NC. (c) TEM image of NC obtained from MnO@NC through the etching of MnO. (d) Schematic illustration of the yolk-shell structure of MnO@NC.

2. TGA curve of MnOS@NSC and XRD pattern after the TGA analysis

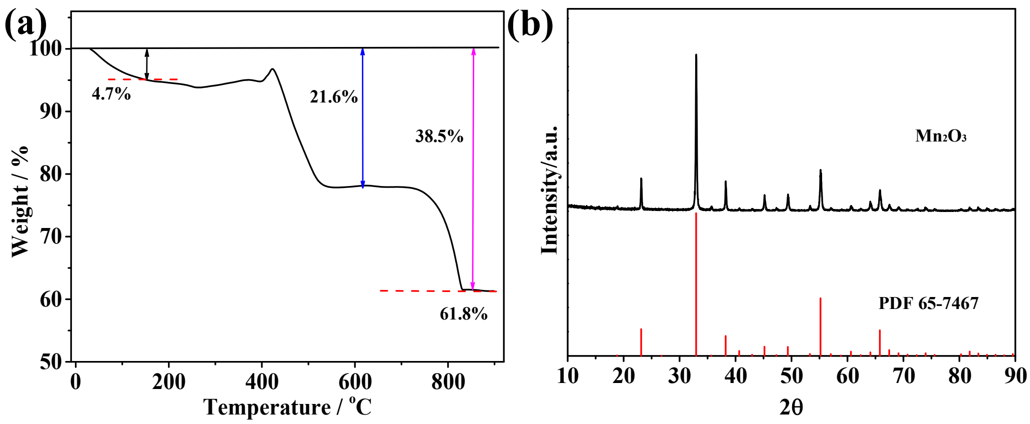

Figure S2. (a) TGA curve of MnOS@NSC, (b) XRD pattern of MnOS@NSC after the TGA analysis.

Calculation of the weight percentage of the NSC in the MnOS@NSC

The weight loss of the MnOS@NSC at the TGA curves in Figure S2a below 150 ºC could be attributed to the removal of physically adsorbed water. The weight increment at 420 ºC can be attributed to the formation of $MnSO_4$ and/or Mn_3O_4 [1] and the subsequent weight loss is the decomposition of the NSC. The weight loss at 700 ºC – 830 ºC is the transformation of $MnSO_4$ and/or Mn_3O_4 to Mn_2O_3. The formation of Mn_2O_3 after the TGA analysis is demonstrated by the XRD pattern in Figure S2b. The content of NSC in the MnOS@NSC (M_{NSC}) can be estimated based on Eq. S2 (where *M* is the weight percentage, *W* is the molecular weight).

$$\frac{2 \times W_{MnOS}}{100 - M_{H_2O} - M_{NSC}} = \frac{W_{Mn_2O_3}}{M_{Mn_2O_3}} \qquad \text{(S1)}$$

3. Raman spectra of MnOS@NSC

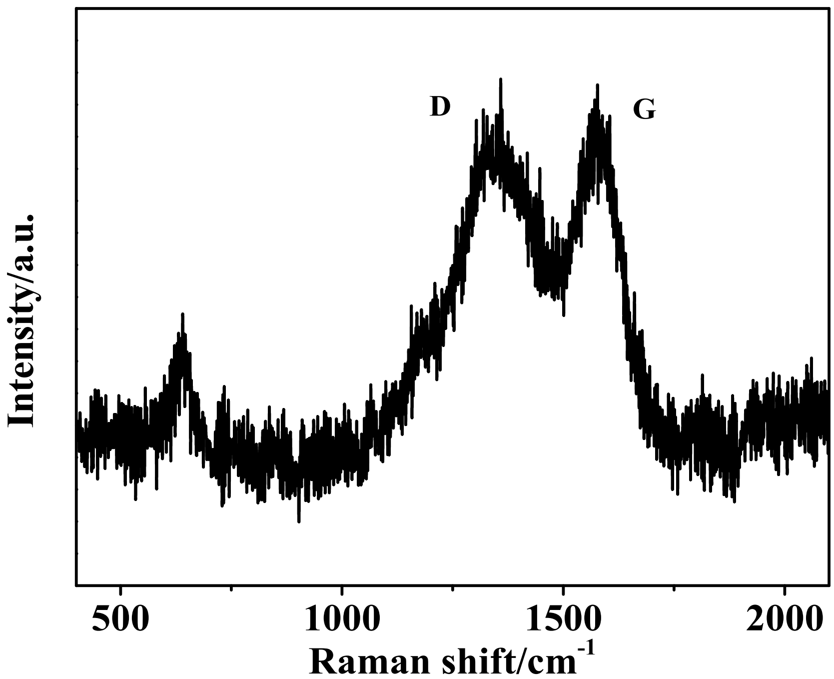

Figure S3. Raman spectra of MnOS@NSC.

4. Rate performance comparison of the MnOS@NSC with other TMO-based anode materials

Table S1. Rate performance comparison of the MnOS@NSC with other TMO-based anode materials.

Samples	mass loading mg cm^{-2}	0.1 A g^{-1}	0.2 A g^{-1}	0.5 A g^{-1}	1.0 A g^{-1}	2.0 A g^{-1}	5.0 A g^{-1}	10. 0 A g^{-1}	Reference
MnOS@NSC	1.5	1339.3	1204.1	1073	928.2	734.7	506.5	290.1	This work
HCF/Mn_3O_4		880	827	750	665	528			2
Mn_3O_4-rGO	1.2	605	480	385	302	198			3
MnO_2@C@ MnO		867.6	709.6	597.1	483.5	387.9			4
m MnO_2-srGO		946.1	852	805	690	643			5
MnO_2/rGO		811	624	394.4	278.2	242.4	168.2		6
MnO_2@HCSO	1.2	792	699	582	495	411	328		7
Porous Mn_2O_3		1012	809	625	509	411	185		8
G/MnO-800	1.5	1000	930	875	762	604			9
MnO@NC	1.0	762	707	643	570	512			10
MnO/RGO		948	817	575	489				11
p-MnO@N-C NTs	1-1.5	945.5	922	859.5	785.7				12
MnO@GS/CNT	1.0	677	600	620	580	530			13
MnO@CNFs	1.2-1.5	817	755	637	520	407			14
MnO@NC		780	650	520	410	335			15
Fe_2O_3/carbon			790	570	450	300		130	16
α- Fe_2O_3-CNFs	1.77	430	385	288					17
Fe_3O_4-C			750	585	518	435	198		18
Fe_3O_4-graphene	1.0	1045		600	410				19
Mesoporous NiO		712	656	607	582	515			20
Porous NiO			510	495	468				21
NiO/C		790		616	461				22
NiO-GNS		1053	1059	967	823				22
CoO-G-C		770	680	570	490	400			23
CoO/C		485	382						24
Co_3O_4/graphene		990	975	805	600				25
Co_3O_4@CNT		789	680	505	453		408		26

5. Electrochemical performance of NSC and NC

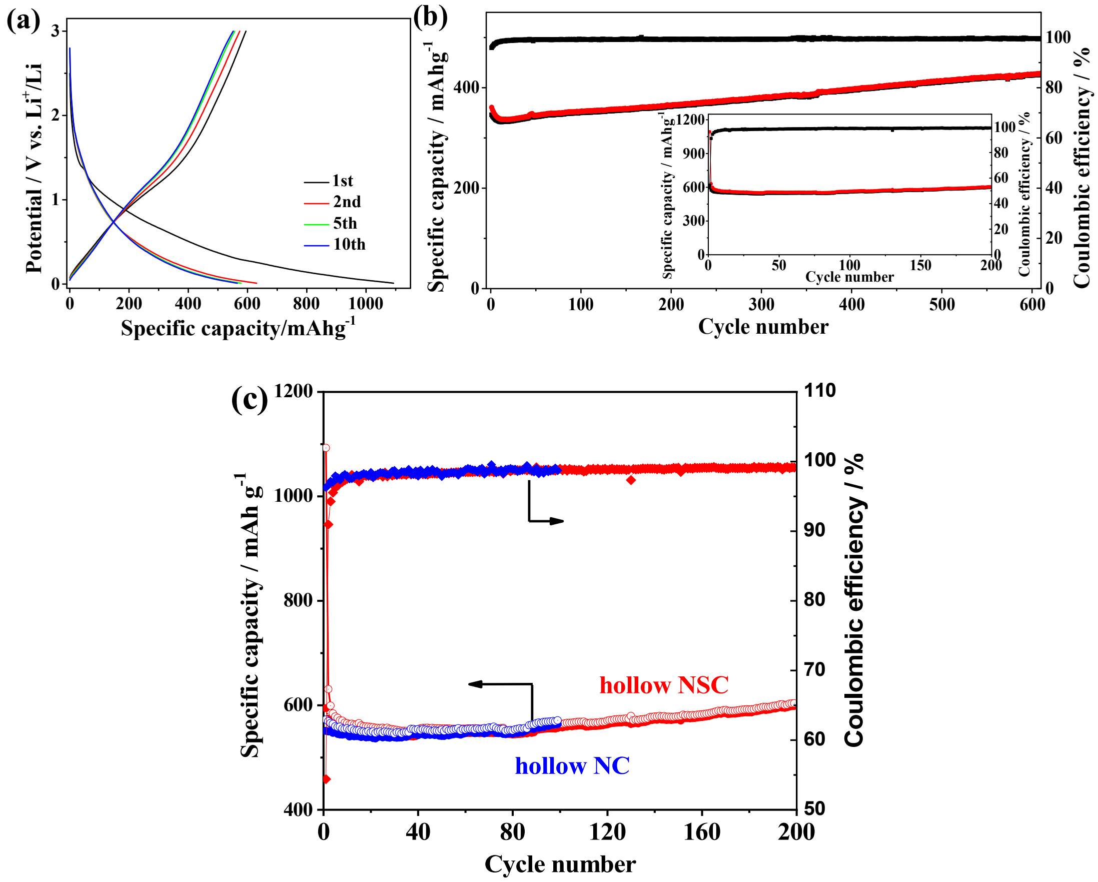

Figure S4. (a) Charge/discharge profiles of the NSC at 100 mA g^{-1}. (b) Cycling performance and Coulombic efficiency of the NSC at 1000 mA g^{-1}. The inset shows the cycling performance and Coulombic efficiency of the NSC at 100 mA g^{-1}. (c) The cycling performance and Coulombic efficiency of the hollow NSC and hollow NC at 100 mA g^{-1}.

6. High resolution XPS spectra of C 1s, O 1s, N 1s, and S 2p in NSC.

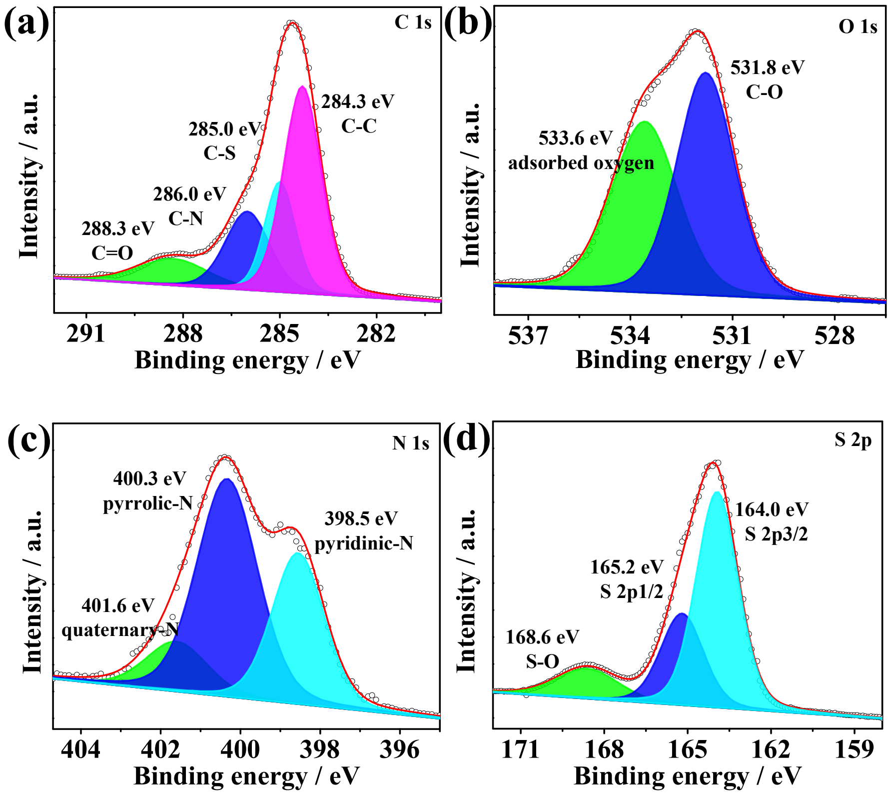

Figure S5. High resolution XPS spectra of (a) C 1s, (b) O 1s, (c) N 1s, and (d) S 2p in NSC.

Table S2. Atomic percentages of C, O, N and S in NSC.

Sample	C (%)	O (%)	N (%)	S (%)
NSC	79.53	11.99	6.89	1.59

7. Total and projected DOSs of MnO_2

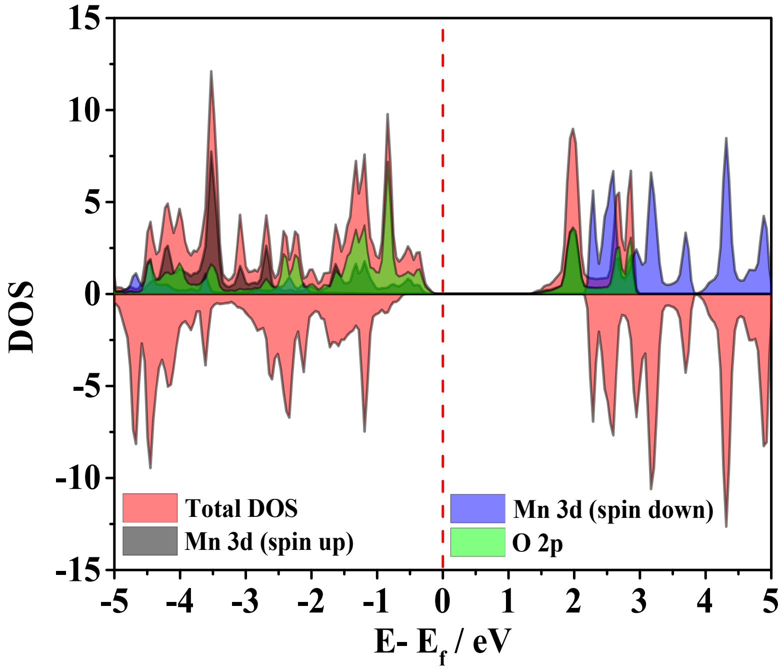

Figure S6. Total and projected DOS of Mn and O atoms.

8. Comparison of the charge transfer resistance of MnOS@NSC with other MnO_2-based electrodes

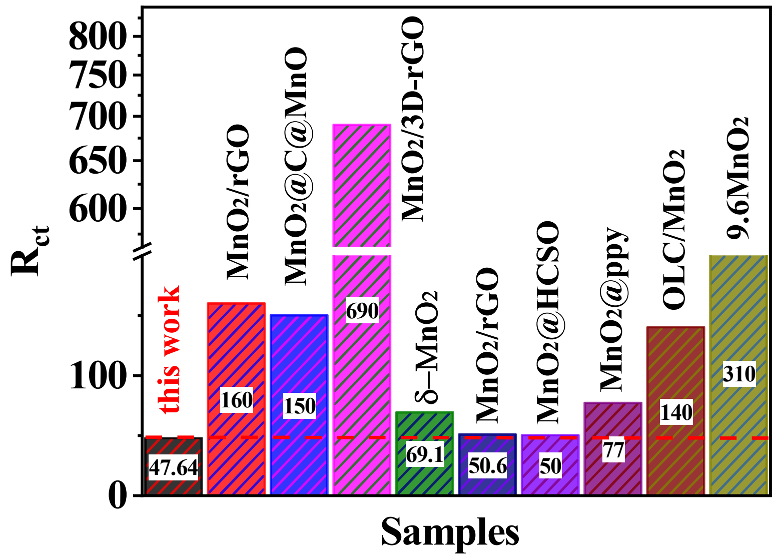

Figure S7. Comparison of the charge transfer resistance with MnO and other MnO_2-

based electrodes.

Table S3. Comparison of the charge transfer resistance with MnO and other MnO_2-based electrodes.

Samples	mass loading mg cm^{-2}	R_{ct}	Reference
MnOS@NC-1	1.5	47.64	This work
MnO_2/rGO	-	160	[27]
MnO_2@C@MnO	-	150	[4]
MnO_2/3D-rGO	-	690	[28]
δ-MnO_2	1.1	69.1	[29]
MnO_2/rGO	-	50.6	[6]
MnO_2@HCSO	1.2	50	[7]
MnO_2@ppy	0.87	77	[30]
OLC/MnO_2	3-4	140	[31]
9.6 MnO_2	1.0	310	[32]
MnO@NC	1.4	100	[33]

References

1. X. Xu, S. Ji, M. Gu and J. Liu, *ACS Appl. Mater. Interfaces*, 2015, **7**, 20957-20964.
2. D. Zhang, G. Li, J. Fan, B. Li and L. Li, *Chem. Eur. J.*, 2018, **24**, 9632-9638.
3. S. P. Varghese, B. Babu, R. Prasannachandran, R. Antony and M. M. Shaijumon, *J. Alloy. Compd.*, 2019, **780**, 588-596.
4. L. Zheng, Y. Liu, J. Lan, Y. Yu and X. Yang, *Chem. Eng. J.*, 2017, **330**, 1289-1296.
5. T. Xu, Q. Meng, Q. Fan, M. Yang, W. Zhi and B. Cao, *Chin. J. Chem.*, 2017, **35**, 1575-1585.
6. A. Aijaz, J. Masa, S. Rösler, W. Xia, P. Weide, A. J. R. Botz, R. A. Fischer, W. Schuhmann and M. Muhler, *Angew. Chem. Int. Ed.*, 2016 **55**, 4087–4091.
7. J. Zang, J. Ye, H. Qian, Y. Lin, X. Zhang, M. Zheng and Q. Dong, *Electrochim. Acta*, 2018, **260**, 783-788.
8. B. Zhang, S. Hao, D. Xiao, J. Wu and Y. Huang, *Mater. Design*, 2016, **98**, 319-323.
9. L. Sheng, S. Liang, T. Wei, J. Chang, Z. Jiang, L. Zhang, Q. Zhou, J. Zhou, L. Jiang and Z. Fan, *Energy Storage Materials*, 2018, **12**, 94-102.
10. G. Zhu, L. Wang, H. Lin, L. Ma, P. Zhao, Y. Hu, T. Chen, R. Chen, Y. Wang, Z. Tie, J. Liu and Z. Jin, *Adv. Funct. Mater.*, 2018, **28**, 1800003.
11. P. Rosaiah, J. Zhu, O. M. Hussain and Y. Qiu, *Ceram. Int.*, 2018, **44**, 3077-3084.
12. D.-S. Liu, D.-H. Liu, B.-H. Hou, Y.-Y. Wang, J.-Z. Guo, Q.-L. Ning and X.-L. Wu, *Electrochim. Acta*, 2018, **264**, 292-300.
13. J. Wang, Q. Deng, M. Li, C. Wu, K. Jiang, Z. Hu and J. Chu, *Nanotechnology*, 2018, **29**, 315403.

14. Y. Guo, L. Zheng, J.-L. Lan, Y. Yu and X. Yang, *Electrochim. Acta*, 2018, **269**, 624-631.
15. Q. Gou, C. Li, W. Zhong, X. Zhang, Q. Dong and C. Lei, *Electrochim. Acta*, 2019, **296**, 730-737.
16. Y. Li, C. Zhu, T. Lu, Z. Guo, D. Zhang, J. Ma and S. Zhu, *Carbon*, 2013, **52**, 565-573.
17. L. Ji, O. Toprakci, M. Alcoutlabi, Y. Yao, Y. Li, S. Zhang, B. Guo, Z. Lin and X. Zhang, *ACS Appl. Mater. Interfaces*, 2012, **4**, 2672-2679.
18. W.-M. Zhang, X.-L. Wu, J.-S. Hu, Y.-G. Guo and L.-J. Wan, *Adv. Funct. Mater.*, 2008, **18**, 3941-3946.
19. P. Lian, X. Zhu, H. Xiang, Z. Li, W. Yang and H. Wang, *Electrochim. Acta*, 2010, **56**, 834-840.
20. H. Liu, G. Wang, J. Liu, S. Qiao and H. Ahn, *J. Mater. Chem.*, 2011, **21**, 3046-3052.
21. C. Wang, D. Wang, Q. Wang and H. Chen, *J. Power Sources*, 2010, **195**, 7432-7437.
22. Y. Xia, W. Zhang, Z. Xiao, H. Huang, H. Zeng, X. Chen, F. Chen, Y. Gan and X. Tao, *J. Mater. Chem.*, 2012, **22**, 9209–9215.
23. M. Zhang, F. Yan, X. Tang, Q. Li, T. Wang and G. Cao, *J. Mater. Chem. A*, 2014, **2**, 5890-5897.
24. W. Yuan, J. Zhang, D. Xie, Z. Dong, Q. Su and G. Du, *Electrochim. Acta*, 2013, **108**, 506-511.
25. H. Kim, D.-H. Seo, S.-W. Kim, J. Kim and K. Kang, *Carbon*, 2011, **49**, 326-332.
26. D. Gu, W. Li, F. Wang, H. Bongard, B. Spliethoff, W. Schmidt, C. Weidenthaler, Y. Xia, D. Zhao and F. Schuth, *Angew.Chem. Int. Ed.*, 2015, **54**, 7060-7064.
27. S. J. Kim, Y. J. Yun, K. W. Kim, C. Chae, S. Jeong, Y. Kang, S. Y. Choi, S. S. Lee and S. Choi, *ChemSusChem*, 2015, **8**, 1484-1491.
28. H. Liu, Z. Hu, Y. Su, H. Ruan, R. Hu and L. Zhang, *Appl. Surf. Sci.*, 2017, **392**, 777-784.
29. A. A. Voskanyan, C.-K. Ho and K. Y. Chan, *J. Power Sources*, 2019, **421**, 162-168.
30. Z. Fan, J. Yan, T. Wei, L. Zhi, G. Ning, T. Li and F. Wei, *Adv. Funct. Mater.*, 2011, **21**, 2366-2375.
31. Y. Wang, Z. J. Han, S. F. Yu, R. R. Song, H. H. Song, K. Ostrikov and H. Y. Yang, *Carbon*, 2013, **64**, 230-236.
32. H. Liu, Z. Hu, H. Ruan, R. Hu, Y. Su, L. Zhang and J. Zhang, *J. Mater. Sci: Mater. Electron.*, 2016, **27**, 11541-11547.
33. Y. Qin, Z. Jiang, H. Rong, L. Guo and Z.-J. Jiang, *Electrochim. Acta*, 2018, **282**, 719-727.